

Article

Evaluating the Impact of Urban Microclimate on Buildings' Heating and Cooling Energy Demand Using a Co-Simulation Approach

Stella Tsoka

Department of Civil Engineering, University of Patras, 26504 Patras, Greece; stsoka@upatras.gr

Abstract: The current research proposes an integrated computational method to consider the effect of the urban microclimate and the higher urban air temperatures on the assessment of urban building energy demands on an annual basis. A one-way coupling procedure is established to generate datasets on typical weather years that can capture the particularities of the urban microclimate as a function of their morphological and geometrical characteristics, thus providing a global perspective of the annual building energy performance at a reasonable computational cost. The proposed simulation method, here applied for an energy performance analysis of generic, non-insulated building units located in four different urban sites of Thessaloniki, Greece, is based on the three tools: (a) the ENVI-met v.4 microclimate model, (b) the Meteonorm weather generator and (c) the dynamic BEPS tool EnergyPlus. The obtained simulation results indicate a decrease in the annual heating energy needs of the examined building units of 8.2–11.5% when the effect of urban warming was accounted for, along with a rise in the annual cooling energy needs of between 13.4 and 28.2%, depending on the case study area.

Keywords: urban microclimate; dynamic building energy performance simulation; ENVI-met; EnergyPlus; typical weather years



Citation: Tsoka, S. Evaluating the Impact of Urban Microclimate on Buildings' Heating and Cooling Energy Demand Using a Co-Simulation Approach. *Atmosphere* **2023**, *14*, 652. <https://doi.org/10.3390/atmos14040652>

Academic Editor: Ferdinando Salata

Received: 20 January 2023

Revised: 15 February 2023

Accepted: 20 March 2023

Published: 30 March 2023



Copyright: © 2023 by the author. Licensee MDPI, Basel, Switzerland. This article is an open access article distributed under the terms and conditions of the Creative Commons Attribution (CC BY) license (<https://creativecommons.org/licenses/by/4.0/>).

1. Introduction

Evaluating building energy demands through dynamic simulation methods necessitates the input of hourly weather data to which the examined building is subjected, which reflect the typical meteorological characteristics over a complete year for a specific geographical location [1]. Generally, a long-term monitoring campaign of various climatic parameters in a specific case study area is not always possible due to time and resource restrictions. To address this limitation, various techniques have been proposed towards the development of typical weather datasets (TWD) that contain the required input parameters for building energy performance simulations [2]. The established procedures generally involve the statistical analysis and processing of multi-year climatic observations that are mainly available from weather stations located in the peripheral zones of cities, such as airports, university campuses, etc. However, climatic records, historically observed in suburban and rural areas, cannot be considered as representative of the conditions occurring in large cities, since the complex interactions between solar radiation (SR), wind speed (WS) and the increased urban densities are not accounted for [3]. In fact, the atmospheric conditions occurring in an urban area are generally characterized by higher air temperatures (T_{air}) compared to those of the surrounding rural areas [4]. The magnitude of urban warming, which varies considerably as a function of time and space, is attributed to various uncontrollable and controllable parameters. While the uncontrollable factors refer to environmental- and nature-related parameters, the controllable ones are mainly related to urban landscape modification, including (a) the reduced urban greenery and the resulting decrease in latent heat flux [5,6], (b) the thermophysical properties of the construction materials that foster heat accumulation and dissipation [7,8], (c) the entrapment of shortwave

and longwave radiation inside street canyons, inhibiting urban cooling [9,10] and (d) the increased anthropogenic heat release as a result of air conditioners, transportation and other human activities [11].

When it comes to estimating the heating and cooling energy demands of an urban building, the hypothesis that the climatic conditions are similar to those of the reference location of a meteorological station (i.e., the airport area) may lead to inaccurate predictions and miscalculations of the building's heating and cooling needs, indicating thus the need to establish more sophisticated approaches in order to capture the particularities of each study area and improve the accuracy of the simulation output. Up to the present time, various methods of different complexity have been proposed towards this direction, combining dynamic BEPS tools either with onsite climatic observations, performed inside the respective study area, or with numerical models for urban microclimate analysis employing computational fluid dynamics (CFD) techniques. Regarding the computational methods, a recent work by Rodler et al. [12] presents an overview of the various co-simulation approaches between urban climate models and building energy models that have been reported in the existing literature, while also discussing their strong and weak points. As stated in the above-mentioned work, many previous scientific studies have coupled the ENVI-met microclimate model with various BEPS tools so as to evaluate the impact of the urban climate on the building's heating and cooling energy demands.

For instance, Yang et al. [13] established an integrated simulation approach between the ENVI-met v.4 microclimate model and the EnergyPlus tool via the software platform Building Controls Virtual Test Bed (BCVTB). Microclimate simulations were performed for a generic case study area in Guangzhou, China, for two typical summer days and obtained hourly climatic records describing the microclimate conditions in front of a building in the case study area were used to modify the existing (epw weather file in the EnergyPlus model). EnergyPlus simulations have also been conducted for the same building under the assumption of an isolated stand-alone case with no surrounding obstacles, and the obtained results were comparatively assessed. It was found that the consideration of the local thermal environment significantly affects the energy performance simulation results, as an increase in the sensible cooling load of around 10% was estimated.

In the same vein, Gobakis and Kolokotsa [3] proposed a combination of the ESP-r dynamic simulation tool with the ENVI-met v.4 model towards an improvement in the accuracy of the energy requirement calculations of a tertiary building in Crete, Greece. The coupling was restricted to four typical days due to the increased computational cost of microclimate simulations. The ENVI-met simulation results were extracted and used to modify the ESP-r hourly weather file for the specific simulated days, while the convective heat transfer coefficient was dynamically estimated in Python. The building's energy performance was evaluated both following the coupling procedure and for the default Meteonorm hourly weather dataset. The analysis suggested a reduction of 2.5% for the heating requirements when the local microclimatic parameters were considered, while an increase in the cooling energy needs ranging between 8.60 and 35% was reported.

Morakinyo et al. [14] proposed a one-way model coupling procedure between ENVI-met and EnergyPlus to examine the role of the urban microclimate and vegetation in the thermal performance of a university building in Nigeria. ENVI-met microclimate simulations were performed for three individual summer days for two cases involving exposed or shaded buildings. The microclimate simulation output was extracted and used to modify the weather profiles in the EnergyPlus tool for the respective summer days. The EnergyPlus simulation outcome revealed significant differences in the indoor thermal environment due to the diverse outdoor microclimatic conditions and the corresponding tree shading effect.

Similarly, Santamouris et al. [15] performed a one-way coupling of the ENVI-met v.4 model with EnergyPlus to assess the impact of various UHI mitigation technologies on the cooling energy requirements of a typical residential building in Sydney. The weather file in EnergyPlus was modified using the microclimate simulation output and the analysis

revealed a decrease in the maximum cooling load of 0.4% for every 10% ground surface albedo increase. On the other hand, for every 10% increase in the urban greenery, a reduction in the peak building cooling load of 0.5–1.0% was found.

Finally, in the study of Tsoka et al. [16], the ENVI-met model was coupled with the EnergyPlus tool to examine the role of street trees on urban building cooling energy demands during a representative summer day. The effects of three tree species with different foliage densities in two different planting patterns were investigated. The obtained simulation results showed that the cooling potential of trees is mainly attributed to radiative shading and the consequent reduction in the solar heat gain, with the most prominent effect being noted for the building units at lower building levels. It can thus be said that taking the microclimatic parameters into consideration during dynamic energy performance simulations will strongly affect the estimated building heating and cooling energy demands. Yet, in the previously mentioned studies, the coupling of microclimate models with dynamic simulation tools is generally conducted for a limited number of days rather than for a complete simulation year, mainly due to the differences in the temporal resolution of the two model categories. Even if significant knowledge on the effect of the local climate on the building's energy demand can be retrieved from a daily analysis, a complete annual simulation would be necessary to obtain a global view of the buildings' energy performance as a function of its surrounding environment.

To address this issue, this study proposes an integrated coupling procedure to generate annual typical weather datasets that capture the particularities of the urban microclimate of urban areas as a function of their morphological and geometrical characteristics. The proposed integrated methodology has been established to achieve both a higher accuracy and computationally efficient dynamic energy performance calculations and it is here applied to an energy performance analysis of generic building units located inside four different urban sites in Thessaloniki, Greece. The procedure is based on three tools: (a) The ENVI-met v.4 microclimate model, (b) the Meteororm weather generator and (c) the dynamic BEPS tool EnergyPlus. More precisely, microclimate simulations with the ENVI-met model are initially performed for all study areas and for 12 representative days (one for each month), defined through a detailed statistical analysis of long-term climatic records. In the second step, the major microclimatic parameters are extracted from ENVI-met and are then introduced in the Meteororm weather generator to stochastically create site-specific annual climatic datasets, henceforward entitled "Urban Specific Weather Datasets" (USWDs). The generated hourly weather datasets, representative of the microclimatic conditions of each one of the four urban sites, will be then used as input boundary conditions for the building unit dynamic energy performance simulations with EnergyPlus.

2. Case Study Areas

The four different urban districts selected for the application of the proposed methodology are located in the city of Thessaloniki, in the northern part of Greece. Following the Köppen climate classification, the climate type of the city is a hot summer Mediterranean climate with generally hot, dry summers; mild, wet winters; and evenly distributed rainfall throughout the year. The four urban districts have a similar size (around 40,000 m²), but they present diverse geometrical and morphological characteristics (i.e., building surface density, height/width ratio (H/W) of the street canyons, green coverage ratio, etc.). In this study and for the sake of clarity, the selected urban districts are named after their main street canyons. The building units, the energy performance of which will be assessed as a function of the local microclimatic conditions, are located in these specific canyons.

The relative locations of the examined case study areas and the location of the meteorological station of the reference location (i.e., the university campus) are shown in Figure 1. Google Earth images of the selected districts and cross-sections of the street canyons in which the examined building units are located are depicted in Figure 2. Buildings in the case study areas are mainly of residential use with very few commercial properties. The building envelope construction materials comprise of cement and concrete elements,

while the ground surfaces are dominated by impervious materials such as asphalt and concrete pavements. The thermal and optical properties of the building envelope and the ground surface materials along with the plant and soil characteristics are provided in the following sections.

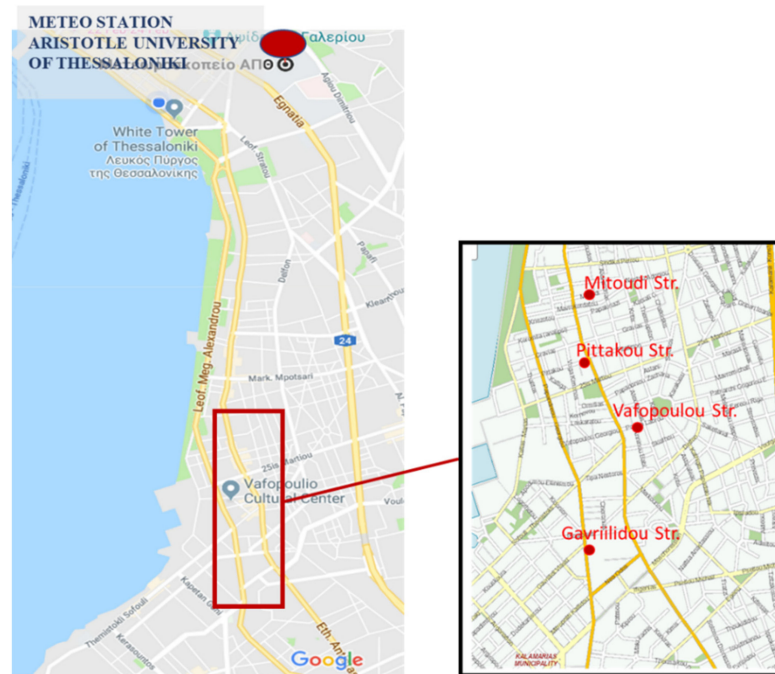


Figure 1. Relative locations of the selected urban districts and the reference location of the meteorological station on the Aristotle University campus.

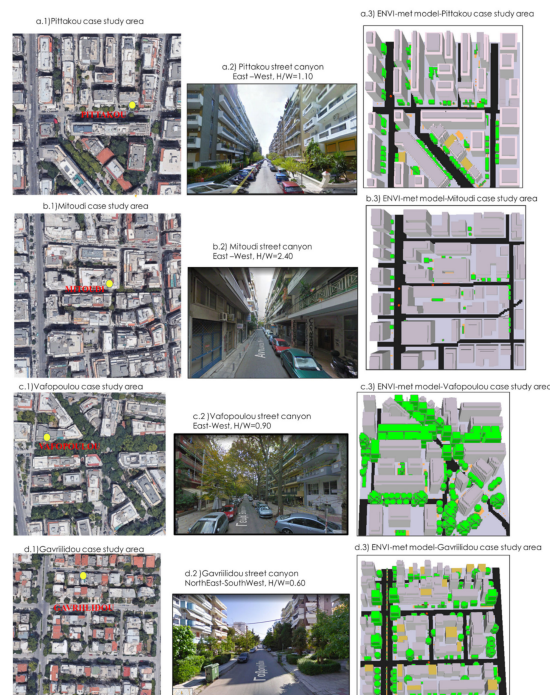


Figure 2. Google Earth images of the selected urban districts and indication of the onsite measurements spot (a.1–d.1), cross-section of the street canyons where the building units, the energy needs of which are to be assessed, are located and an indication of their orientation and H/W ratio (a.2–d.2) and the 3D ENVI-met area input files of the case study areas (a.3–d.3).

3. Materials and Methods

As previously mentioned, the current research aims to combine dynamic building energy simulation tools and microclimate models to account for the local microclimate conditions in the calculation of annual building heating and cooling energy requirements. As suggested in the existing literature, the generation of typical weather files requires several years of meteorological data [17]; thus, for the creation of the USWDs, microclimate simulations for various years would be required, a suggestion that is practically temporally inconceivable. The above-mentioned limitation indicates the need to follow a different approach, which is summarized by the following: instead of simulating several years, 12 representative days, one for each month, are simulated in the ENVI-met model and the urban specific weather datasets are generated from the obtained microclimate results.

To this aim, the current study uses the Meteororm tool, a synthetic yearly weather generator that uses stochastic methodologies to create time series of hourly data. The generation of a synthetic weather year in Meteororm can be performed after the introduction by the user of the monthly averages of the most important weather variables (i.e., dry bulb temperature, relative humidity (RH), global radiation and wind speed). In the second step, daily and hourly values are stochastically generated with intermediate data with the same statistical properties as the monthly imported data, i.e., average value, variance and characteristic sequence. In this study, for the urban specific weather datasets (USWDs), the required average values are provided by the simulated climatic data of the selected 12 representative days, which are defined following a detailed statistical analysis of the relevant long-term climatic data.

The idea of simulating the microclimatic parameters of 12 representative days and introducing the respective outcome into synthetic weather generators to obtain annual weather datasets has been previously described and implemented by Oxizidis et al. [18] in the Atrous project. However, given the time restrictions, the authors did not have sufficient time to conduct a sound statistical analysis of the definition of the 12 representative days, leading to some abnormalities in the obtained annual weather datasets. To address this issue, in this study, the representative days are defined according to a detailed statistical analysis of long-term climatic parameters and the respective procedure is further described in the methodology section.

In parallel with the development of the USWDs, a “Reference Weather Dataset” (RWD), corresponding to the reference location of a meteorological station, is also created. In this study, the respective reference location is the meteorological station of the Department of Meteorology and Climatology, located on the campus of the Aristotle University of Thessaloniki. Contrary to the USWDs, the generated “reference” weather file could be theoretically used for every study area inside the city; no specific microclimatic conditions of each case study area are considered. Again, for the generation of the RWD, the Meteororm stochastic weather generator is used, and the necessary climatic averages are issued from the multiyear measured data of the meteorological station. The energy performance of generic residential building units will be then assessed for the created USWDs, reflecting the microclimatic conditions in their vicinity, and the RWD using the EnergyPlus dynamic simulation model. As further described in the following sections, the models of the four study areas are created in ENVI-met and EnergyPlus, with special attention to make sure surfaces are properly described and that a proper exchange of data between the two tools is achieved.

Finally, a comparative analysis of the obtained heating and cooling loads will provide further insight into (a) the energy penalty due to different climatic conditions in the urban areas (comparison of USWDs and RWD) and (b) the impact of the local site-specific microclimatic conditions on building heating and cooling energy requirements (comparison among the four USWDs). The various steps of the implemented methodology are shown in Figure 3.

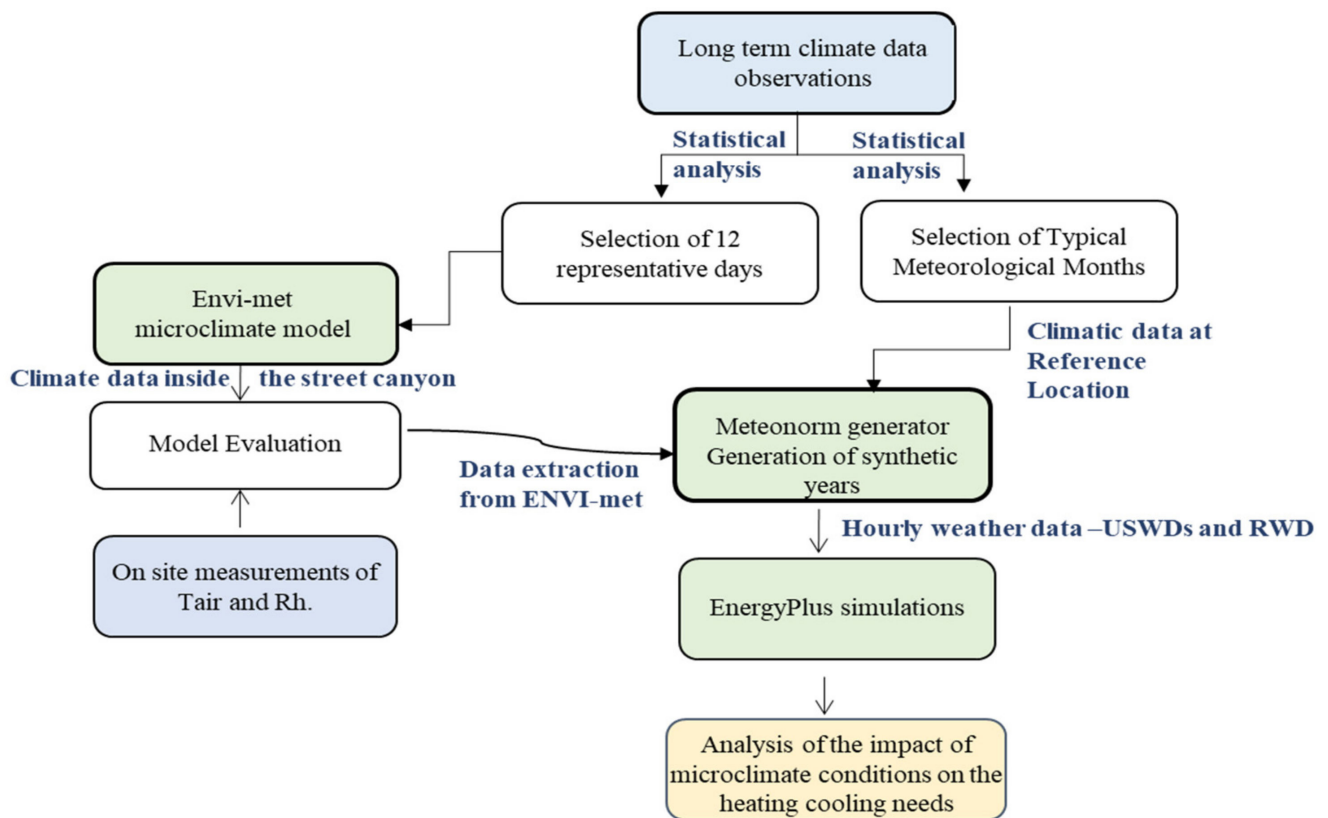


Figure 3. Flow chart of the implemented methodology.

3.1. Onsite Monitoring Campaign

In order to obtain the necessary data for the evaluation of the ENVI-met microclimate model, onsite microclimatic measurements of air temperature (Tair) and relative humidity (RH) were conducted in all four study areas using high accuracy weatherproof HOBO data loggers suitable for the outdoor environment. According to the logger manufacturer, the accuracy of the Tair sensor is ± 0.21 °C for records varying from 0.0 °C to 50.0 °C, while for the relative humidity sensor, the accuracy is $\pm 2.5\%$ for the corresponding measurements ranging from 10% to 90%. To assure the precision of the measurements and avoid any issues related to reflected solar radiation, the loggers were placed inside suitable radiation shields that can be also mounted on tripods, masts or flat vertical surfaces. Given that the microclimatic measurements had to be conducted for a long period, the monitoring equipment was placed on the balconies of buildings in the study areas, away from potential risks such as theft, damage, etc. Microclimatic monitoring took place over a year, from September 2015 to September 2016, and the sensors recorded the air temperature and relative humidity at intervals of 1 h.

The different mounting procedures of the loggers at each one of the respective study areas are shown in Figure 4, whereas the locations of the loggers are shown in Figure 2a.1–d.1 (yellow spot). In the Pittakou and Gavriilidou study areas, the radiation shields were mounted on tripods, while in the Mitoudi and Vafopoulou case study areas, they were mounted on vertical flat rigid surfaces, fixed accordingly to remain stable. To eliminate potential boundary effects formed along the building walls, the radiation shields were placed at a minimum distance of 60.0 cm from the exterior building walls.

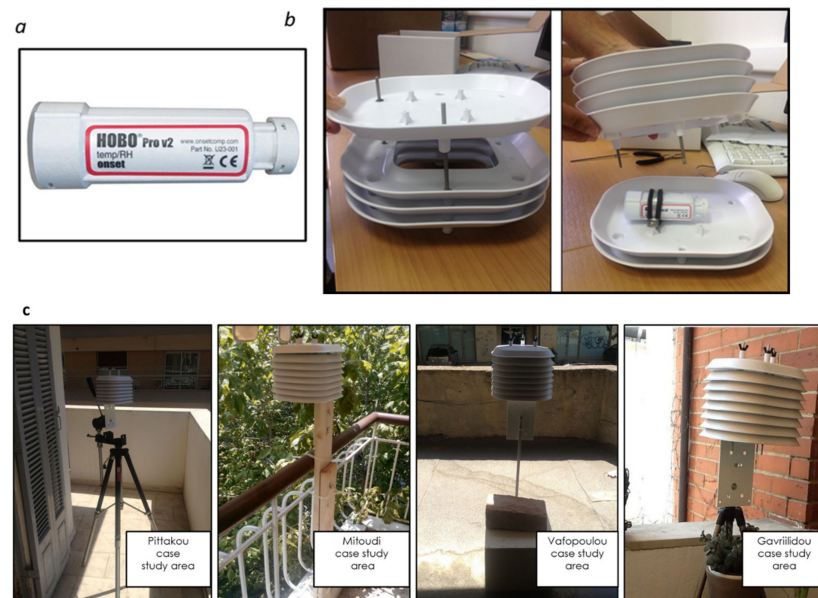


Figure 4. (a) Weatherproof HOBO data loggers suitable for the outdoor environment, (b) radiation shields in which the loggers were placed and (c) mounting of the radiation shields at each one of the four study areas.

3.2. Long-Term Climatic Data for the Definition of the Representative Days and the Selection of the Typical Meteorological Months

Generating typical climate datasets necessitates the analysis of long-term observations of various climatic variables. Thus, both for the USWDs and the RWD, multiyear climatic observations are necessary. For this study, two sets of multiyear measured data, recorded at the meteorological station on Aristotle University campus were available. The first dataset corresponds to the ten year period of 1993–2003 and contains monthly average values of air temperature, relative humidity, wind speed (WS) and solar radiation (SR), while the second dataset corresponds to the 42 year period of 1958–2000 and contains daily average Tair values. The first dataset (i.e., 1993–2003) was used to define the typical meteorological months, the average values of which were then introduced into the Meteonorm weather generator to obtain the RWD. On the other hand, the second database was applied to define the representative days for which the ENVI-met microclimate simulations will be performed, and the corresponding microclimatic outcome will be used for the creation of the USWDs. A detailed procedure for the selection of typical meteorological months and representative days is described in [19,20], whereas the respective final selection is depicted in Tables 1 and 2. At this point, the following remark should be made: theoretically, the representative days could have been selected from any calendar year; however, the reason that they were selected from the time period September 2015–2016 lies in the fact that onsite measurements of Tair and RH, necessary for the evaluation of the ENVI-met model, were performed during this specific period.

Table 1. Typical meteorological months for the city of Thessaloniki and the corresponding average monthly values of solar radiation (SR), air temperature (Tair), dew point temperature (Tdew) and wind speed (WS) introduced into the Meteonorm weather generator.

Typical Month	SR (kWh/m ²)	Tair °C	Tdew °C	WS m/s
January 1995	44.47	5.78	4.07	2.18
February 1997	63.78	7.63	5.39	2.04
March 2000	103.91	9.33	6.79	2.02
April 2001	115.86	14.26	11.72	1.67

Table 1. Cont.

Typical Month	SR (kWh/m ²)	Tair °C	Tdew °C	WS m/s
May 2002	145.48	19.60	16.12	1.57
June 2000	164.64	24.20	20.61	1.92
July 1994	165.10	26.67	23.03	1.9
August 2001	155.60	27.60	23.57	1.69
September 2000	115.50	21.78	17.66	1.57
October 2003	78.96	17.34	15.00	1.63
November 1997	43.02	11.80	10.10	1.30
December 2003	41.93	7.60	5.87	1.81

Table 2. Selected representative days for the city of Thessaloniki and the corresponding air temperature (Tair) deviations from the respective long-term median values.

Selected Representative Day	Deviation	Selected Representative Day	Deviation
4 January 2016	7%	22 July 2016	0.7%
8 February 2016	11%	10 August 2016	5.5%
28 March 2016	2.7%	24 September 2016	0.6%
21 April 2016	1.8%	1 October 2015	1.8%
16 May 2016	2%	26 November 2015	3.3%
1 June 2016	1.1%	20 December 2015	2.7%

3.3. Set-Up of the ENVI-Met Microclimate Simulations

In this study, ENVI-met v.4 was used for microclimate simulations conducted for the 12 representative days and for all the four case study areas (48 ENVI-met simulations in total). The ENVI-met model is designed to simulate complex surface–vegetation–air interactions in the urban environment, and it is based on the fundamental laws of fluid dynamics and thermodynamics. It can simulate the diurnal cycle of major climatic variables, such as air and soil temperature and humidity, wind speed and direction, radiative fluxes, etc., with a typical horizontal resolution between 0.5 m and 5.0 m and a time step of 1 to 5 s [21]. The model’s detailed characteristics along with the mathematical equations governing the various sub-models and the shortcomings and limitations of the model are provided in the scientific work of Huttner [21] and Simon [22] as well as in the literature review of Tsoka et al. [23]. In this study, all the examined districts had an area of 200 m × 200 m. For their modelling, a set of 134 × 134 grids was adopted for the x and y axis with a resolution of 1.5 m, while in the z axis, the number of cells was set to 20 with a 3.0 m resolution. To minimize the boundary effects and improve the numerical stability of the model, seven nesting grids were placed around the main domain area. Building floors are considered to have a height of 3.0 m, whereas the height of the base floor was set to 4.5 m. Moreover, in all four case study areas, buildings were mostly constructed before 1980, prior to any thermal regulation. The building envelope components were thus considered as non-insulated. The thermal and optical properties of the building envelope and ground surface materials are presented in Tables 3 and 4, respectively.

To increase the accuracy of the microclimate simulations, special attention was paid to a precise representation of the geometric and foliage characteristics of the vegetation species present in each one of the four case study areas. In the first two case study areas (i.e., Pittakou and Mitoudi), the dominant plant types are the evergreen *citrus aurantium* and the deciduous *hibiscus syriacus* and *robinia pseudoacacia*, whereas in the Vafopoulou area, the vegetation species mainly comprise the deciduous *acer negundo* and *platanus orientalis*. Finally, in the fourth case study area, all the above-mentioned deciduous and evergreen tree types are present. The 3D profiles of the above-mentioned plants were created in the “Albero” database in the ENVI-met model to enhance the accuracy of the simulated surface–plant–air interaction. Simple 1D plants were considered for the grass areas. The

height and width of the plants were defined according to onsite measurements provided in [26], and the respective adopted values are given in Table 5.

Table 3. Thermal and optical properties of the building envelope materials.

Material	Thickness (m)	Thermal Conductivity (W/mK)	Albedo ¹ (%)
Plaster	0.02	0.87	40
Brick	0.19	0.51	-
Concrete slab	0.15	2.5	-
Roof tiles	0.03	1.5	30

¹ Defined only for the exterior layers of the building envelope components.

Table 4. Thermal and optical properties of the ground surface materials [24,25].

	Volumetric Heat Capacity (J/m ³ K)	Thermal Conductivity (W/mK)	Albedo ¹ (%)
Asphalt	2.1×10^6	0.70	12
Concrete tiles	2.1×10^6	1.50	30
Loamy soil	3.0×10^6	1.45	20

¹ Defined only for the exterior layers of the building envelope components.

Table 5. Height and crown diameter of the modeled tree species.

Title 1	Acer Negundo	Platanus Orientalis	Hibiscus Syriacus	Robinia Pseudoacacia	Citrus Orientalis
Height (m)	2.0	7.0	3.5	8.0	3.5
Crown diameter (m)	8.0	5.0	2.0	4.0	3.0

To continue, the leaf area density, a parameter reflecting the foliage characteristics of the modeled tree types, must be defined at different intervals heights, while also accounting for its seasonal variation for deciduous tree types [27]. However, in the existing literature, relevant LAD measurements are mainly available in summer, when the peak foliage density has been reported [28–30]. On the other hand, the seasonal variation in the foliage characteristics has rarely been investigated using on-site experimental campaigns [31], and thus there is insufficient knowledge on the LAD values during defoliation periods.

Based on the results of the experimental campaigns, trees with a very dense crown have LAD values close to $2.0 \text{ m}^3/\text{m}^2$, while in the cases of dense and porous crowns, the respective LAD values reach $1 \text{ m}^3/\text{m}^2$ and $0.7 \text{ m}^3/\text{m}^2$ [29–32]. Other studies have also established empirical relationships between the foliage density of the respective species and the interception of direct solar radiation [33]. In the present study, and based on the existing evidence, the species of *Robinia pseudoacacia*, *Acer negundo* and *Platanus orientalis* are considered as trees with a very dense crown, with a maximum LAD of $2.0 \text{ m}^3/\text{m}^2$, while *Hibiscus syriacus* is considered to have a dense crown with a peak LAD of $1.0 \text{ m}^3/\text{m}^2$.

For the evergreen *Citrus aurantium*, a very dense crown is also considered. In terms of the LAD variability throughout the year and given that the deciduous trees follow a similar temporal profile of foliation and defoliation phases, the adopted values are based on the experimental campaign of Öztürk [31]. The foliation period is thus considered to start at the end of March and reaches peak values in May; for the months of April and May, 50% and 100% LAD_{max} are considered, correspondingly. A stable foliage density period, expanding from May to mid-September, is then considered, and then the defoliation period begins. A reduction of 50% and 70% in the LAD_{max} is assumed for the months of October and November, correspondingly, while from December to March, a minimum LAD reaching only 10% of the LAD_{max} is assumed. The respective temporal profiles and the considered LAD values that were introduced into the Albero Database are displayed in Figure 5.

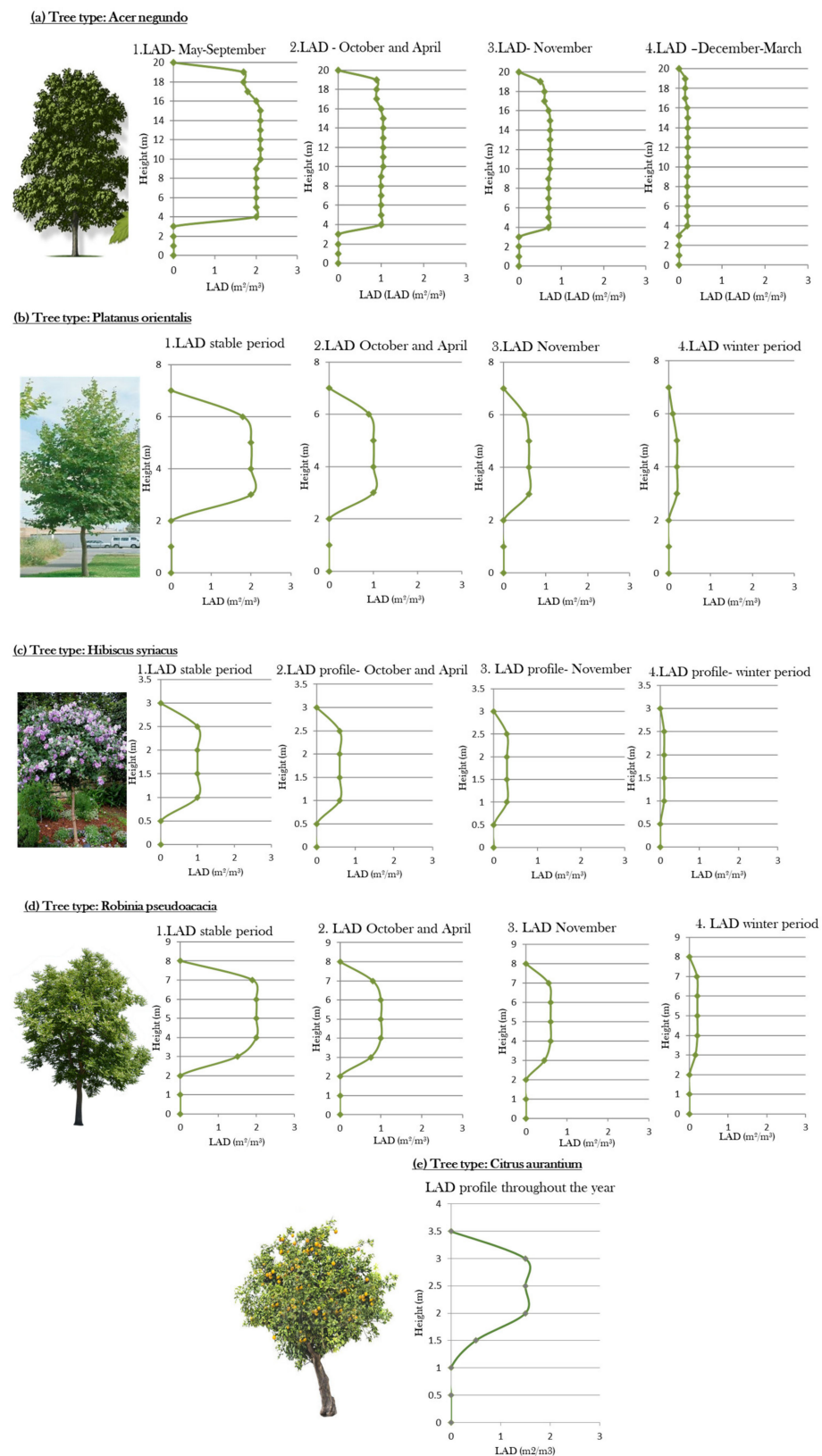


Figure 5. Seasonal variation in the LAD profile for all tree species of the examined areas.

To finalize the model set-up, in all four study areas, receptors points were placed at the corresponding field measurements points and also near the façades of the building units so as to evaluate the ENVI-met model. The energy performance of these receptor points will also be assessed. Based on the recommendations of Yang et al. [13], five receptor

points providing microclimatic values of air temperature, relative humidity, wind speed, shortwave radiation, etc., were placed 0.75 m away from the buildings' façades.

In the next step, the necessary meteorological boundary conditions are defined. As previously mentioned, for each representative day, four simulations were carried out (one for each area) with the meteorological boundary conditions remaining the same, only the area input file was different. Thus, the differences in the acquired microclimatic outputs will only be due to the diversity of the urban morphology. All microclimate simulations were conducted for a 24 h cycle, starting from 00:00 and ending at 23:59, while the output interval for all result files was set to 30 min.

The basic parameters of the simulations are the average daily wind speed at 10 m height, the wind direction during the simulated day, the hourly values of air temperature and the relative humidity, along with the mean monthly value of soil temperature. In this study, all the above-mentioned parameters were obtained from the meteorological station of Aristotle University, located on the university campus. A summary of the meteorological conditions used in the model is provided in Table A1 and Figure A1 of Appendix A. However, since there were no available data on soil humidity, the default ENVI-met values were considered (i.e., 50% moisture content for the upper soil layer and 60% for the middle and deep soil layers). The solar adjustment factor was always equal to 1 to avoid further modifications of the estimated shortwave radiation fluxes. In all microclimatic simulations, clear sky conditions were considered, an assumption based on the observations of the meteorological conditions during the selected representative days. Finally, the default 1.5 Order E- ϵ closure model was applied in the turbulence model and a roughness length of 0.1 m was set for all simulation days and case study areas.

3.4. Extraction of Microclimate Data and Generation of the USWDs

Once the microclimate simulations were complete, the respective microclimatic output was extracted and used to generate the site-specific weather datasets. In the current research, the case study building units are located on the 1st and 3rd floors. The ground floor of the analyzed buildings, in which the examined building units are contained, has a height of 4.5 m and the typical building floors have a height of 3.0 m. Moreover, the main façade is exposed to exterior conditions, while the ground surface, ceiling and the rest of the vertical façades are considered as adiabatic due to the same operational schedules between the apartments. Based on the above-mentioned remarks, for the 1st floor and 3rd floor building units, the microclimate simulation results for each simulation day were extracted for the heights of 4.5 m and 7.5 m and 10.5 m and 13.5 m, correspondingly, the obtained values were then averaged and the acquired averages were used as input data for the MeteorNorm weather generator to create site-specific weather datasets for each study area and for each building floor.

3.5. Configuration of the Dynamic Energy Performance Simulations

In this study, a total of 16 EnergyPlus simulations were conducted for each one of the four case study areas. The energy performance of the building units of the 1st and 3rd floor was simulated using (a) the reference weather dataset (RWD), that could be theoretically used for every site in the city of Thessaloniki (1st run) and (b) the corresponding site-specific weather dataset (i.e., the generated USWDs), reflecting the climatic conditions in the vicinity of the examined building unit (2nd run). All simulations were performed for the existing building envelopes, in which there is no thermal insulation. A plan of the assumed building unit with a total surface area of 90 m² and the respective 3D model introduced into the EnergyPlus tool are depicted in Figure 6. The generic apartment is designed as a single thermal zone and it is surrounded by other neighboring apartments on the same floor, while the staircase area is assumed to be an unconditioned thermal zone (no thermostatic control). The main façade of the building unit is exposed to the exterior conditions, while the vertical façade separating the apartment from the staircase is exposed to an unconditioned thermal zone. The floor, ceiling and the rest of the vertical

facades of the apartment are considered as adiabatic due to the same operational schedules between apartments.

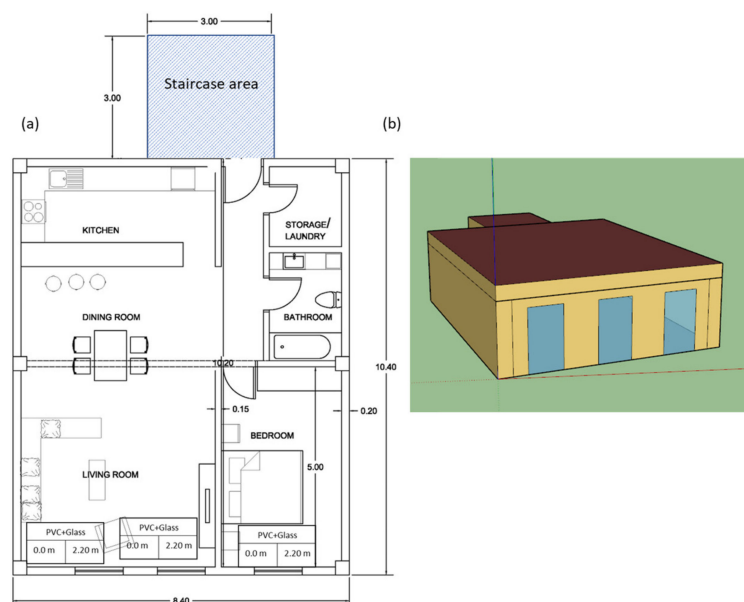


Figure 6. Plan of the typical building unit (a) and the corresponding 3D model (b).

Regarding the thermal properties of the examined building units, the opaque external building wall consists of brick masonry, with $U = 1.64 \text{ W/m}^2\text{K}$, and the bearing vertical components of reinforced concrete present U values between $2.53 \text{ W/m}^2\text{K}$ and $3.17 \text{ W/m}^2\text{K}$, depending on their width. For the sake of consistency, the thermal properties and the width of the building envelope components considered in EnergyPlus were the same as those considered in the ENVI-met model. The brick wall and the reinforced concrete components exposed to the non-conditioned staircase area present U values of $1.43 \text{ W/m}^2\text{K}$ and $2.06\text{--}2.46 \text{ W/m}^2\text{K}$, respectively. In terms of the windows, their thermal transmittance is $U = 2.8 \text{ W/m}^2/\text{K}$ and they are assumed to have double-glazed glass and a synthetic frame. The interior wall partitions and the concrete slab of each of the examined building units are considered as internal mass objects with a total surface area of 260 m^2 , which is the same both for the 1st and the 3rd floor building units. Finally, the operational schedules of the generic building units, including occupancy, lighting, equipment, ventilation, heating and cooling setpoints and the infiltration rates, were defined according to the national regulatory framework for building energy performance [34].

Finally, all the surrounding buildings of the street canyons in which the examined building units are located were represented as shading objects. To assure simulation consistency, the height of the shading objects, the width of the balconies and the distance of the opposite buildings were identical to those in the corresponding 3D geometrical model of the ENVI-met tool. However, they were only accounted for as shading objects in the Vafopoulou street canyon, particularly the vegetation elements; in the rest of the case studies, either there was no vegetation in front of the investigated building units (i.e., in Mitoudi) or the vegetation only consisted of low bushes, presenting no shading effect on the analyzed apartments (i.e., Pittakou and Gavriilidou canyons). Given that the deciduous trees in Vafopoulou street have an unstable foliage density throughout the year, a specific schedule for the tree transmittance was created in the EnergyPlus model, with values based on the respective LAD values considered in the ENVI-met simulations. More precisely, in the EnergyPlus model, only variations in the light transmission factor were considered for the trees as shading objects. Based on the results of previous studies, correlating the foliage density with the fraction of light transmitted through the foliage [33], the following assumptions have been made: The maximum LAD values, reported from May

to September, correspond to a minimum light transmission of 6%, while the minimum LAD values, reported from December to March, correspond to a maximum light transmission of 90%. Intermediate LAD values in April and October correspond to a light transmission of 50%, while the respective value in November was set to 70% (see Figure 5 for LAD annual distribution). Figure 7 shows the surrounding obstacles for all the examined 1st and 3rd floor building units.

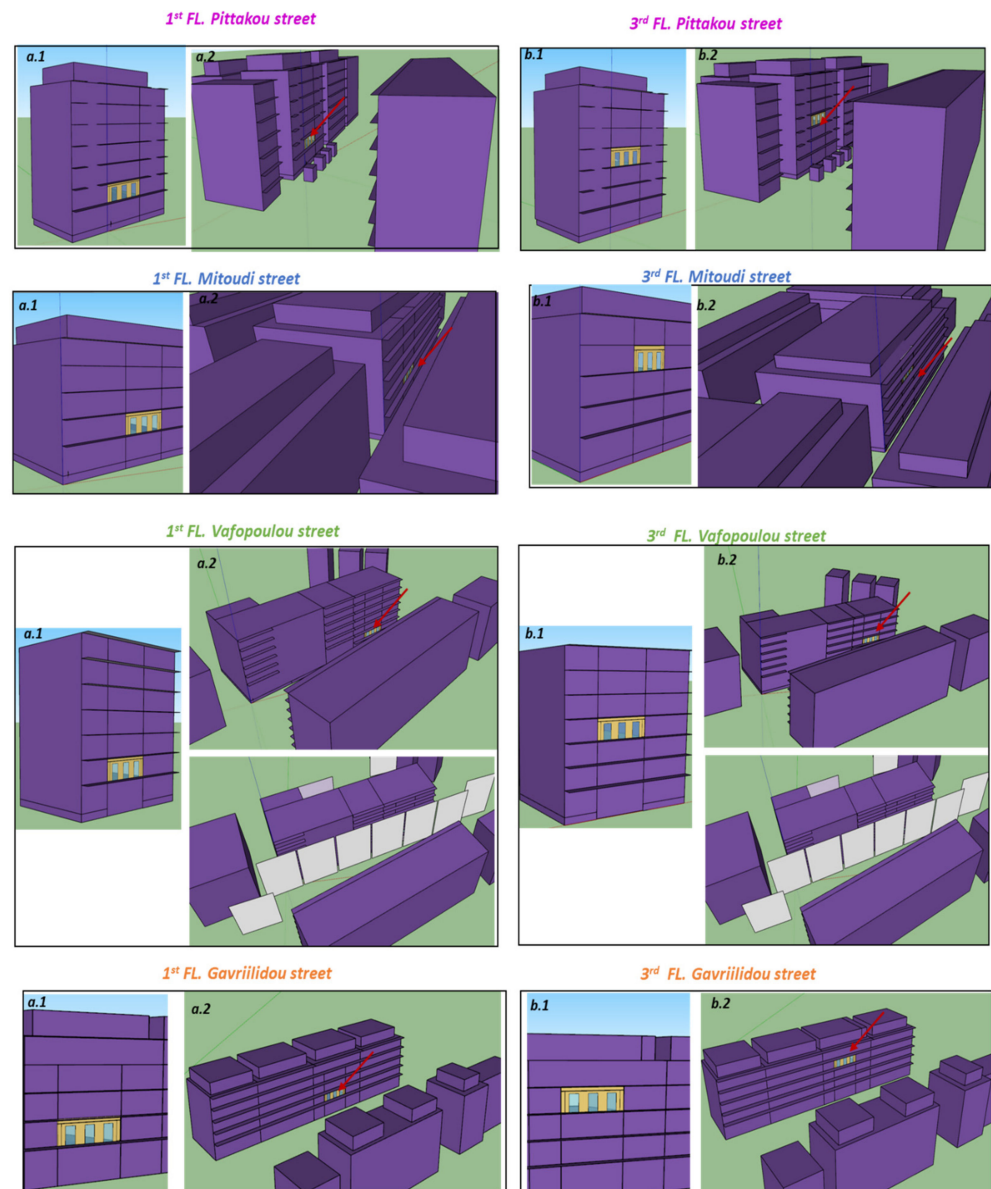


Figure 7. Indication of the location of the investigated building units in the building (a.1,b.1 for the 1st and 3rd floor building units, respectively) and position of the surrounding building obstacles (a.2,b.2 for the 1st and 3rd floor building units, respectively).

4. Results

4.1. Evaluation of the ENVI-Met Microclimate Model

In the first step, the reliability of the ENVI-met model to accurately predict the local microclimatic conditions is assessed. Following the existing literature, the model's evaluation is conducted through the estimation of statistical metrics such as the root mean square error (RMSE) (Equation (1)), the mean bias error (MBE) (Equation (2)), the mean absolute error (MAE) (Equation (3)) and the index of agreement, d (Equation (4)). The

estimated values were then compared with the respective error values that are reported in the literature. Here, the assessment of the model’s accuracy is performed for the parameters of air temperature and relative humidity, as due to a limitation of resources, the onsite monitoring of surface temperature and mean radiant temperature was not possible.

$$RMSE = [N^{-1} \sum_{i=1}^N (Pi - Oi)^2]^{1/2} \tag{1}$$

$$MBE = N^{-1} \sum_{i=1}^N (Pi - Oi) \tag{2}$$

$$MAE = N^{-1} \sum_{i=1}^N |Pi - Oi| \tag{3}$$

$$d = 1 - [\sum_{i=1}^N (Pi - Oi)^2 / \sum_{i=1}^N (|Pi - \overline{O}| + |Oi - \overline{O}|)^2] \tag{4}$$

Pi: value predicted by the model

Oi: measured value

To assure the model’s accuracy under different seasonal variations, the selected different metrics were initially estimated for one representative day of each season. The observed data of Tair and RH were acquired through the monitoring campaign described in Section 3.1, and the calculated values for all four study areas are shown in Table 6. In all the examined case study areas and for all seasons, the estimated quantitative metrics are always within the range of the respective accepted values already reported in the literature [23]. More precisely, concerning the Tair simulation results, in three out of the four case study areas, the model was found to overestimate part of nighttime temperatures and underestimate part of daytime Tair values during spring and summer.

Table 6. Estimated difference metrics for all case study areas and for all seasons.

		RMSE		d		MAE		MBE	
		Tair (°C)	RH (%)						
Pittakou study area	Spring	1.14	6.70	0.93	0.90	0.95	2.50	−0.64	2.85
	Summer	1.02	10.24	0.94	0.97	0.82	7.70	−0.24	−7.60
	Autumn	1.55	4.80	0.65	0.98	1.50	3.50	−1.23	−0.85
	Winter	0.85	4.70	0.70	0.97	0.78	4.30	−0.78	4.20
Mitoudi study area	Spring	1.19	7.30	0.98	0.95	1.05	6.70	−0.70	3.30
	Summer	1.35	12.0	0.97	0.65	1.19	11.0	−0.74	11.5
	Autumn	1.15	5.35	0.70	0.95	1.11	4.61	−1.14	−4.70
	Winter	1.35	9.80	0.65	0.82	1.28	9.70	−1.15	9.74
Vafopoulou study area	Spring	1.13	5.60	0.92	0.94	1.0	4.90	−0.67	7.10
	Summer	0.95	3.70	0.98	0.97	0.80	3.04	−0.69	−1.06
	Autumn	1.35	3.17	0.97	0.98	1.29	2.23	−1.29	−1.99
	Winter	1.11	5.98	0.61	0.95	1.05	5.70	−1.01	5.50
Gavriilidou study area	Spring	0.95	4.35	0.92	0.89	0.90	3.40	−0.90	−1.5
	Summer	0.89	10.05	0.96	0.90	0.70	8.20	−0.10	−7.0
	Autumn	1.27	12.0	0.92	0.70	1.15	8.50	−0.20	−6.0
	Winter	0.91	6.80	0.77	0.95	0.80	6.50	−0.70	4.80

On the other hand, in all four case study areas, the model always underestimated the winter Tair values, and in three out of the four case study areas, the model always underpredicted the Tair values in autumn. In terms of the relative humidity results, the analysis suggested that in three out of the four case study areas, the model always overestimated the relative humidity values during spring, whereas in all four case study areas, the model always overestimated the winter RH values. On the other hand, in three

out of the four case study areas, the ENVI-met model always underpredicted the diurnal RH values in summer due to not accounting for the sea breeze effect, and in all four study areas, the model tended to underestimate the values of RH during autumn.

Based on the previous remarks, the ENVI-met model can be considered as a reliable tool for microclimate simulations under different meteorological conditions. Microclimate simulations for the rest of the representative days were then conducted to acquire the necessary microclimatic data for the creation of the urban specific weather files. As previously mentioned, a total of 48 ENVI-met microclimate simulations were performed (i.e., for each of the twelve representative days for the four case study areas) and the hourly microclimatic outputs in front of the examined building units are extracted and processed as described in Section 3.4. to obtain the USWDs that will be further used for dynamic energy performance simulations.

4.2. Comparison of the Generated Annual Weather Datasets for the 1st Floor Building Units

In this section, the acquired stochastically generated climatic data are further analyzed and compared. More precisely, the Tair values of the generated USWDs are compared with the respective values of the RWD to assess potential differences occurring because of the urbanization and the induced urban warming. In parallel, the climatic parameters of the USWDs are compared with each other so as to evaluate the impact of the differentiated urban morphology on the local microclimatic conditions. The comparative analysis was carried out for both the USWDs of the 1st and 3rd floor building units.

The evolution of the daily and monthly mean Tair values are shown in Figure 8. As it can be seen, the estimated Tair values, both for the USWDs and the RWD, follow a similar inter-annual profile, with the latter generally presenting lower Tair values. This is due to the position of the meteorological station of the University inside a park area with increased vegetation, lower building density and thus cooler microclimatic conditions. The range of the daily Tair varies between $-1.4\text{ }^{\circ}\text{C}$ and $31.1\text{ }^{\circ}\text{C}$, $-1.4\text{ }^{\circ}\text{C}$ and $30.7\text{ }^{\circ}\text{C}$, $-1\text{ }^{\circ}\text{C}$ and $30.2\text{ }^{\circ}\text{C}$ and $-1.4\text{ }^{\circ}\text{C}$ and $31.2\text{ }^{\circ}\text{C}$ for the USWDs of Pittakou, Mitoudi, Vafopoulou and Gavriilidou, respectively, while the corresponding range for the RWD is $-1.5\text{ }^{\circ}\text{C}$ to $30.4\text{ }^{\circ}\text{C}$. In all the examined datasets, the maximum and minimum daily values were found in mid-August and mid-January, respectively.

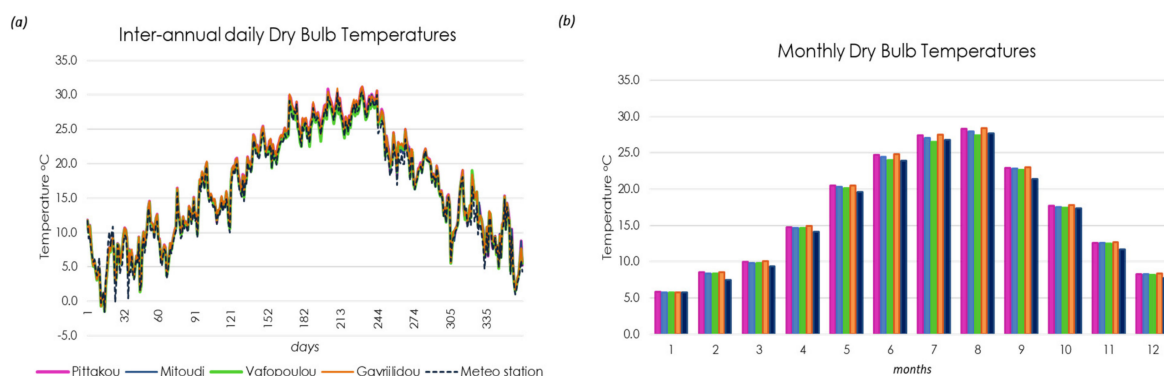


Figure 8. (a) Inter-annual daily dry bulb temperatures and (b) the mean monthly values of Tair for the urban specific weather datasets corresponding at the 1st floor building units inside the four urban canyons and the reference weather dataset over a typical year.

In the next step, the mean monthly Tair values estimated for the four USWDs were compared with the corresponding values of the reference weather file. In all cases, the predicted values inside the urban canyons were generally higher compared to the reference area. The only exception was noted in the Vafopoulou area, where the monthly Tair value in July and August was lower than that of the meteorological station by around $0.3\text{ }^{\circ}\text{C}$ due to the very high vegetation coverage and its consequent positive effects. For all areas, smaller deviations are found in January, while in September, the monthly Tair for the

USWDs of Pittakou/Mitoudi/Gavriilidou is 1.5 °C, 1.4 °C and 1.6 °C higher than that of the meteorological station. In addition, in Gavriilidou canyon, the monthly Tair values in May, June and July are 0.9 °C, 0.85 °C and 0.7 °C higher than those of the reference location, whereas for the building unit in Mitoudi, the corresponding deviations are 0.7 °C, 0.5 °C and 0.3 °C.

Furthermore, the Tair differences among the four USWDs are attributed to their diverse morphological and geometrical characteristics, affecting the exposure to solar radiation, the wind speed, the convective heat losses, etc. While in winter only marginal differences are found due to the low solar altitude and the low solar radiation intensity of this period, during summer, the deviations are of higher significance. In fact, the mean monthly Tair value in front of the 1st floor building unit in Vafopoulou canyon is 1.0 °C lower than the corresponding value in Gavriilidou canyon both in July and August, due to the high solar interception by the dense tree foliage. Similar deviations, close to 1.0 °C, are also noted between Vafopoulou and Pittakou street canyons. In the latter, the south facing façade of the 1st floor building unit receives direct radiation from 7:00 a.m. to 17:00 p.m., since the moderate aspect ratio of the canyon did not provide any shading of the 1st floor level and the vegetation is not high enough to assure efficient shading of the building surfaces.

4.3. Comparison of the Generated Annual Weather Datasets for the 3rd Floor Building Units

The evolution of the average daily and monthly Tair values throughout the year estimated in the near vicinity of the 3rd floor building units of the four study areas and for the reference location are shown in Figure 9. As it can be seen, in all cases, a similar inter-annual profile is noted; the ranges of the daily Tair values vary between 1.5 and 31.0 °C, −1.5 and 30.8 °C, −1.5 and 29.4 °C and −1.5 and 30.9 °C for the USWDs of Pittakou, Mitoudi, Vafopoulou and Gavriilidou, respectively, marginally different from the respective values of the 1st floor building units.

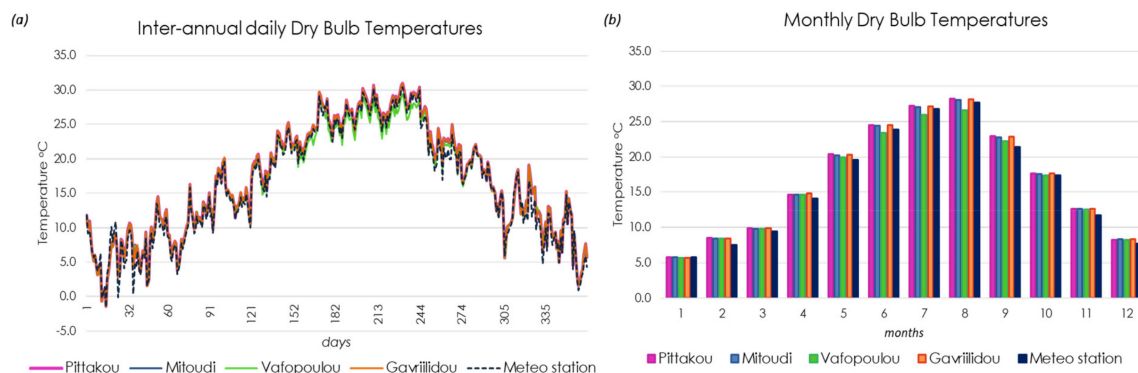


Figure 9. (a) Inter-annual daily dry bulb temperatures and (b) the mean monthly values of Tair for the urban specific weather datasets corresponding at the 3rd floor building units inside the four urban canyons and the reference weather dataset over a typical year.

Moreover, the Tair values at the reference location of the meteorological station are generally lower compared to those found for the urban areas. For the heating period, the maximum deviations were noted in February, when the monthly Tair values in front of the 3rd floor building unit in Pittakou, Mitoudi and Gavriilidou area are 1.0 °C, 0.90 °C and 0.95 °C higher than the Tair at the meteorological station (i.e., 13.0%, 12.0% and 12.6% higher). On the other hand, in August, the Tair values near the building units in Pittakou and Gavriilidou canyons are almost 2% higher than the corresponding reference value (i.e., close to 0.50 °C higher), whereas in Mitoudi canyon, the estimated deviation from the Tair of the meteorological station is slightly lower (i.e., 0.37 °C).

Finally, a comparison of the mean monthly Tair results of the four USWDs leads to the following remarks: The deviations in the estimated monthly Tair values in front of the 3rd floor building units in Pittakou, Mitoudi and Gavriilidou case study areas are

negligible throughout the year. Indicatively, the monthly Tair difference between Pittakou and Mitoudi in summer does not exceed 0.2 °C, whereas in winter, it is close to 0.05 °C. Similarly, the Tair differences in front of the building units in Mitoudi and Gavriilidou are lower than 0.15 °C. In the above-mentioned canyons, the façades of the examined 3rd floor building are exposed to solar radiation for a similar duration and for the majority of the day in summer; however, the Tair in Mitoudi canyon is slightly lower. This is due to the high aspect ratio of the Mitoudi canyon, contributing to solar obstruction of most of the ground and the building surfaces of the lower levels, leading to smaller amounts of reflected solar radiation reaching the examined building unit and also to a lower sensible heat release from the canyons’ surfaces. As result, the warming of the air layer near the investigated building façade in Mitoudi canyon is of smaller significance compared to Pittakou and Gavriilidou streets. On the other hand, during July and August, the Tair in front of the 3rd floor building unit in Vafopoulou canyon is 1.2 °C and 1.5 °C, respectively, lower than the corresponding values in Gavriilidou canyon. This is due to the important contribution of tree foliage to the reduction in direct solar radiation reaching the buildings and ground surfaces of the Vafopoulou street canyon, since they are mostly kept in shadow throughout the day by the dense tree foliage. Similar deviations exceeding 1.3 °C are also noted between Vafopoulou and Pittakou street canyons in summer.

4.4. Dynamic Energy Performance Simulation Results

The simulation outputs of the annual energy needs of the investigated building units of the 1st and 3rd floor are depicted in Figure 10. The simulation results of each building unit are presented in pairs, involving the annual heating and cooling energy needs estimated for the corresponding USWD and the RWD. In terms of the total thermal energy, the analysis suggested a 3–8.5% and 3.9–12.7% higher energy demand for the 1st and 3rd floor building units, respectively, when the RWD was used instead of the site-specific weather file. In addition, the simulation results indicate that the use of the RWD instead of the respective USWD leads not only to an underestimation of the cooling energy needs but also to an overestimation of the heating energy demand due to the neglect of the urban warming effect.

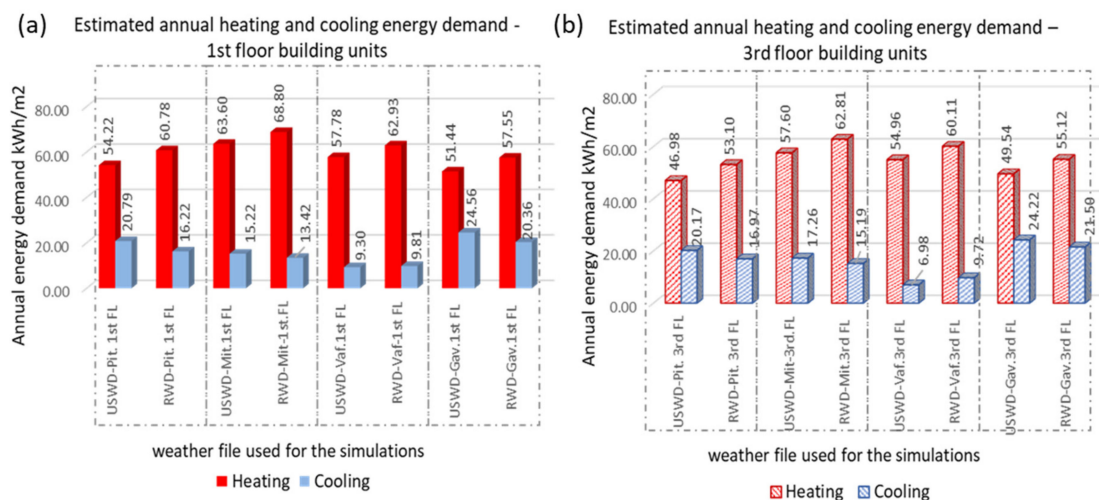


Figure 10. Estimated annual heating and cooling energy demands using the RWD and the USWDS for (a) the examined 1st floor building units and (b) the 3rd floor building units.

In fact, the heating energy needs for the 1st floor building units in Pittakou and Mitoudi street canyons were 10.8% and 7.6% lower when the respective USWDs were used as weather datasets for the simulations rather than the RWD, while the corresponding percentage deviations for Vafopoulou and Gavriilidou building units were 8.2% and 10.6%. Similarly, for the examined 3rd floor building units, the estimated annual heating energy

demand using the RWD outweighs the respective heating energy needs calculated with the USWDs by 11.5%, 8.3%, 8.6 and 10.1% for the 3rd floor apartments in Pittakou, Mitoudi, Vafopoulou and Gavriilidou streets, respectively. The above-mentioned findings agree with the results of previous relevant studies, investigating the positive effect of the higher ambient urban T_{air} on building's heating energy needs [35,36].

However, even if the higher urban T_{air} values contribute to a reduction in the heating energy requirements, this is not the case for the estimated cooling energy needs of all the examined building units. In fact, the higher ambient T_{air} values inside the urban areas result in an increase in the annual cooling energy needs for the 1st floor building units in Pittakou, Gavriilidou and Mitoudi canyons by 28.2%, 20.6% and 13.4%, respectively, compared to the estimated energy demand for the RWD. It has to be mentioned that in the Mitoudi canyon, the percentage deviation is lower due to the lower summer T_{air} difference between the Mitoudi street and the reference location. More precisely, during the cooling period (i.e., May–September), the average difference between the T_{air} near the façade of the 1st floor building unit in Mitoudi and the meteorological station is 0.55 °C, while the corresponding differences for Pittakou and Gavriilidou study areas reach 1.0 °C. It can thus be said that the high aspect ratio of the Mitoudi street canyon and the consequent control of the solar gains of the building unit's façade led to a lower energy penalty of urban warming.

Similarly, the annual cooling energy needs of the 3rd floor building units in Pittakou, Gavriilidou and Mitoudi canyons are higher when the microclimatic conditions are accounted for compared to the corresponding values obtained for the RWD; the respective percentage deviations reach 18.9%, 13.6% and 12.7%, respectively, highlighting again the importance of considering the local microclimatic parameters when a high accuracy of dynamic building energy performance simulations is required. Nevertheless, the reverse trend has been noted in Vafopoulou; the cooling energy needs for the 1st and 3rd floor building units are 5% and 28%, respectively, lower when the local microclimatic conditions are considered compared to the corresponding values for the RWD. This differentiation is attributed to the significantly high presence of vegetation in this specific urban area, resulting in very low solar gains during summer and in an increased latent heat release by the tree foliage, which results in cooling of the ambient air of the urban area. The latter parameters have been captured by the ENVI-met model; thus, the average summer T_{air} values (i.e., June–August) reported using the USWD for the 1st and 3rd floor building units in Vafopoulou street are 26.0 °C and 25.4 °C, whereas the corresponding average summer T_{air} using the RWD is 26.1 °C (see also Section 3). It can thus be said that the high presence of vegetation in the Vafopoulou area contributed to improved microclimatic conditions that are closely similar to the conditions of the reference location of the meteorological station.

5. Conclusions and Discussion

The current study aimed to apply a computational method combining dynamic building energy performance simulation (BEPS) tools with microclimatic models to accurately evaluate building annual heating and cooling energy needs. Typical hourly weather datasets were created to be representative of the microclimatic conditions occurring in the vicinity of generic 1st and 3rd floor building units located in four urban areas in Thessaloniki.

The obtained results revealed the importance of applying an integrated coupling method between microclimatic models and dynamic building energy simulation tools to capture the particularities of the local microclimate of each study area and improve the accuracy of the dynamic energy performance simulations. For all the examined building units, the analysis revealed the beneficial impact of the higher ambient urban T_{air} values on the reduction in the annual heating energy needs, an effect that is strongly counterbalanced in summer, given the significant rise in building cooling energy needs. The annual heating energy needs of the examined building units were found to be 8.2–11.5% lower when the site-specific microclimate data were considered rather than the climatic data from the

reference location. On the other hand, the higher T_{air} values in the urban districts captured in the USWDs resulted in a rise in the annual cooling energy needs of between 13.4% and 28.2%, depending on the study area. A comparison of the energy performance simulation results of the 1st and 3rd floor building units located in the same building (calculated with the use of their respective USWDs) generally suggested lower heating energy needs for the apartments at a higher level. This is mainly due to the higher solar gains of the thermal envelope, rather than the air temperature differences near the facades. The annual heating energy needs of the examined 3rd floor building units were found to be 3.7–13.4% lower than the corresponding estimated energy demands of the 1st floor building units.

Furthermore, a comparison of the energy performance simulation results of the 1st and 3rd floor building units estimated using the respective USWDs revealed the considerable role of the morphological and geometrical characteristics of the four urban areas, since parameters such as the aspect ratio and vegetation presence strongly affected both the thermal gains transmitted into the thermal zones and the T_{air} value in the vicinity of the examined building units. The estimated differences in the annual heating energy needs of the examined building units ranged between 5 and 18%. However, the effect of different solar gains was found to be more prominent for the estimated cooling rather than for the heating energy needs. The most significant differences among the investigated building units were noted between the 1st and 3rd floor apartments in Gavriilidou and Vafopoulou street canyons, which received the highest and the lowest direct solar radiation during summer, respectively. In the latter canyon, the annual cooling energy demands of the 1st and 3rd floor building units were lower than the respective needs of the Gavriilidou street units by almost a factor of three.

To conclude, as mentioned in the Introduction, most studies that employ co-simulation approaches between energy performance simulations and microclimate models have mainly focused on the summer period and a respective estimation of the cooling energy needs. However, the contribution of the current research lies in the extension of microclimate simulations and the corresponding improvements in typical weather datasets (TWDs) in order to examine the effect of the local microclimate, not only on the cooling needs, but also on the heating energy demands, thus providing a global perspective of the annual building energy performance at a reasonable computational cost.

Still, there are some restrictions of this study that should be taken into consideration during the results analysis. As mentioned in the methodology section, the representative days were selected here according to a statistical analysis of long-term daily T_{air} values; long-term climatic records including daily average WS and RH values were not available. Thus, the definition of the 12 representative days was only limited to the T_{air} parameter. As suggested in [19], this restriction could lead to the selection of representative days that present either very high wind speeds due to potential wind gusts or very calm wind speed conditions. Even if the wind speed is also extracted by the ENVI-met model to generate the USWDs in the Meteonom weather generator, to eliminate potential inaccuracies in terms of the convective heat losses in the EnergyPlus simulations, the internal and external convective heat transfer coefficients are described by a static value, according to the procedure of the ISO 6946 [37]. More precisely, the standard parameters assume a constant wind speed value of 4m/s for the estimation of the exterior convective heat transfer coefficient, a value that outweighs the respective values encountered inside the dense urban street canyons and estimated in the ENVI-met model; still, under this assumption, the estimation of the energy performance of the building units using the reference weather dataset and the corresponding site-specific weather dataset will be conservative. To address this issue, the acquisition of long-term daily climatic parameters, including not only the mean daily T_{air} , but also the WS, RH and SR, would be necessary.

Moreover, to reduce the computational cost, this study conducted microclimate simulations for 12 representative days—one for each month—and the obtained microclimatic values were averaged and introduced into the Meteonom weather generator. The hourly values were then stochastically generated with intermediate data with the same statisti-

cal properties as the mean imported data, i.e., average value, variance and characteristic sequence. The reason that this approach was followed was primarily due to reducing the computational cost; simulating complete months in the ENVI-met model and using the respective hourly outcomes to modify the typical weather files for the city of Thessaloniki would have undoubtedly provided results of higher accuracy [38]. However, simulations for 12 complete months for four case study areas at a high horizontal spatial resolution of $1.5 \text{ m} \times 1.5 \text{ m}$ would require a large amount of computational time and increased computational power and thus, this option was eliminated for this study.

Future research should involve further efforts to reduce the computational cost of the established computational approach; a sensitivity analysis involving the simulation of the study areas at different scales and different resolutions could be performed. If the smaller simulation domains and the smaller grid resolution do not compromise the accuracy of the microclimatic output, the respective model configuration could be adopted and further used for the microclimatic analyses of the 12 representative days and the generation of the USWDs. Moreover, a future research direction could also involve the application of the presented computational approach in buildings of various typologies built in different climatic zones.

Funding: This research received no external funding.

Data Availability Statement: The data presented in this study are available on request from the corresponding author.

Acknowledgments: This study was conducted for the PhD thesis of the corresponding author [20], who would also like to thank the Department of Meteorology and Climatology, School of Geology, of the Aristotle University of Thessaloniki, Greece, for their support of this work.

Conflicts of Interest: The author declares no conflict of interest.

Appendix A

Table A1. Input boundary conditions for ENVI-met microclimate simulations.

	Representative Day	WS at 10 m (m/s)	WD	Soil Temp. Upper Layer (K)	Soil Temp. Middle Layer (K)	Soil Temp. Deep Layer (K)
Spring period	28 March 2016	2.75	WSW	284.3	285	293
	21 April 2016	5.40	WNW	289	289.6	293
	16 May 2016	3.90	WSW	295	295.5	293
Summer period	1 June 2016	1.23	SW	306	304.8	293
	22 July 2016	1.15	SW	305.5	304.5	293
	10 August 2016	1.20	SW	305	304	293
Autumn period	24 September 2015	1.73	SW	299	300	293
	1 October 2015	2.30	SW	292	293	293
	26 November 2015	1.28	SW	286	287	293
Winter period	20 December 2015	1.15	SW	281.5	282.5	290
	4 January 2016	1.30	SW	280.3	282	290
	8 February 2016	1.90	WSW	279.5	281.5	290

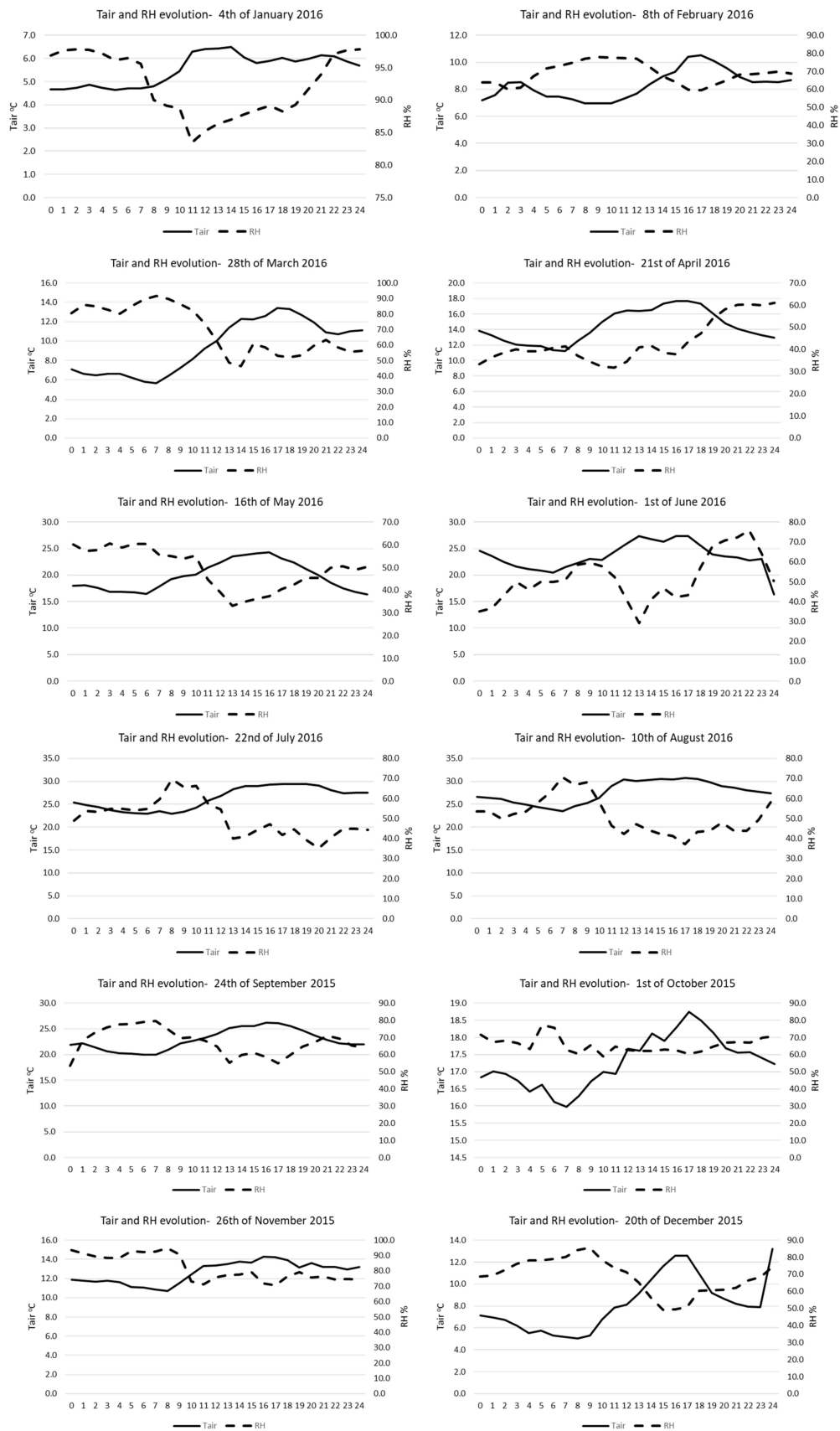


Figure A1. Hourly Tair and RH values as input boundary conditions for microclimate simulations of the 12 representative days.

References

1. Crawley, D.B. Which weather data should you use for energy simulations of commercial buildings? *ASHRAE Trans.* **1998**, *104*, 498.
2. Seo, D.; Huang, Y.J.; Krarti, M. Impact of Typical Weather Year Selection Approaches on Energy Analysis of Buildings. *ASHRAE Trans.* **2010**, *116*, 416–427.
3. Gobakis, K.; Kolokotsa, D. Coupling building energy simulation software with microclimatic simulation for the evaluation of the impact of urban outdoor conditions on the energy consumption and indoor environmental quality. *Energy Build.* **2017**, *157*, 101–115. [[CrossRef](#)]
4. Oke, T.R. City size and the urban heat island. *Atmos. Environ.* **1973**, *7*, 769–779.
5. Taha, H. Urban climates and heat islands: Albedo, evapotranspiration, and anthropogenic heat. *Energy Build.* **1997**, *25*, 99–103. [[CrossRef](#)]
6. Akbari, H.; Cartalis, C.; Kolokotsa, D.; Muscio, A.; Pisello, A.L.; Rossi, F.; Santamouris, M.; Synnefa, A.; Wong, N.H.; Zinzi, M. Local climate change and urban heat island mitigation techniques—the state of the art. *J. Civ. Eng. Manag.* **2016**, *22*, 1–16. [[CrossRef](#)]
7. Santamouris, M. Using cool pavements as a mitigation strategy to fight urban heat island—A review of the actual developments. *Renew. Sustain. Energy Rev.* **2013**, *26*, 224–240. [[CrossRef](#)]
8. Santamouris, M. Regulating the damaged thermostat of the cities—Status, impacts and mitigation challenges. *Energy Build.* **2015**, *91*, 43–56. [[CrossRef](#)]
9. Oke, T.R. The energetic basis of the urban heat island. *Q. J. R. Meteorol. Soc.* **1982**, *108*, 1–24. [[CrossRef](#)]
10. Oke, T.R. Street design and urban canopy layer climate. *Energy Build.* **1988**, *11*, 103–113. [[CrossRef](#)]
11. Ohashi, Y.; Genchi, Y.; Kondo, H.; Kikegawa, Y.; Yoshikado, H.; Hirano, Y. Influence of air-conditioning waste heat on air temperature in Tokyo during summer: Numerical experiments using an urban canopy model coupled with a building energy model. *J. Appl. Meteorol. Climatol.* **2007**, *46*, 66–81. [[CrossRef](#)]
12. Rodler, A.; Lauzet, N.; Musy, M.; Azam, M.H.; Guernouti, S.; Mauree, D.; Colinart, T. Urban microclimate and building energy simulation coupling techniques. In *Urban Microclimate Modelling for Comfort and Energy Studies*; Springer: Cham, Switzerland, 2021; pp. 317–337.
13. Yang, X.; Zhao, L.; Bruse, M.; Meng, Q. An integrated simulation method for building energy performance assessment in urban environments. *Energy Build.* **2012**, *54*, 243–251. [[CrossRef](#)]
14. Morakinyo, T.E.; Dahanayake, K.K.C.; Adegun, O.B.; Balogun, A.A. Modelling the effect of tree-shading on summer indoor and outdoor thermal condition of two similar buildings in a Nigerian university. *Energy Build.* **2016**, *130*, 721–732. [[CrossRef](#)]
15. Santamouris, M.; Haddad, S.; Saliari, M.; Vasilakopoulou, K.; Synnefa, A.; Paolini, R.; Ulpiani, G.; Garshasbi, S.; Fiorito, F. On the energy impact of urban heat island in Sydney: Climate and energy potential of mitigation technologies. *Energy Build.* **2018**, *166*, 154–164. [[CrossRef](#)]
16. Tsoka, S.; Leduc, T.; Rodler, A. Assessing the effects of urban street trees on building cooling energy needs: The role of foliage density and planting pattern. *Sustain. Cities Soc.* **2021**, *65*, 102633. [[CrossRef](#)]
17. Costanzo, V.; Evola, G.; Infantone, M.; Marletta, L. Updated typical weather years for the energy simulation of buildings in mediterranean climate. A case study for sicily. *Energies* **2020**, *13*, 4115. [[CrossRef](#)]
18. Oxizidis, S.; Dudek, A.V.; Papadopoulos, A.M. A computational method to assess the impact of urban climate on buildings using modeled climatic data. *Energy Build.* **2008**, *40*, 215–223. [[CrossRef](#)]
19. Tsoka, S.; Tolika, K.; Theodosiou, T.; Tsikaloudaki, K.; Bikas, D. A method to account for the urban microclimate on the creation of ‘typical weather year’ datasets for building energy simulation, using stochastically generated data. *Energy Build.* **2018**, *165*, 270–283. [[CrossRef](#)]
20. Tsoka, S. Urban Microclimate Analysis and Its Effect on the Buildings’ Energy Performance. Ph.D. Thesis, Aristotle University of Thessaloniki, Thessaloniki, Greece, 2019.
21. Huttner, S. Further Development and Application of the 3D Microclimate Simulation ENVI-met. Ph.D. Thesis, Mainz University, Mainz, Germany, 2012.
22. Simon, H. Modeling urban microclimate: Development, Implementation and Evaluation of New and Improved Calculation Methods for the Urban Microclimate Model ENVI-met. Ph.D. Thesis, Mainz University, Mainz, Germany, 2016.
23. Tsoka, S.; Tsikaloudaki, A.; Theodosiou, T. Analyzing the ENVI-met microclimate model’s performance and assessing cool materials and urban vegetation applications—A review. *Sustain. Cities Soc.* **2018**, *43*, 55–76. [[CrossRef](#)]
24. *ISO 10456:2007*; Building Materials and Products-Hygrothermal Properties-Tabulated Design Values and Procedures for Determining Declared and Design Thermal Values. International Organization for Standardization: Geneva, Switzerland, 2007.
25. *ISO 13370:2007*; Thermal Performance of Buildings-Heat Transfer via the Ground-Calculation Methods. International Organization for Standardization: Geneva, Switzerland, 2007.
26. Kontogianni, A. The Impact of Urban Green Structure and Composition on the Climate of the Cities. Ph.D. Thesis, Aristotle University of Thessaloniki, Thessaloniki, Greece, 2017.
27. Salata, F.; Golasi, I.; de Lieto Vollaro, R.; de Lieto Vollaro, A. Urban microclimate and outdoor thermal comfort. A proper procedure to fit ENVI-met simulation outputs to experimental data. *Sustain. Cities Soc.* **2016**, *26*, 318–343. [[CrossRef](#)]

28. Gillner, S.; Vogt, J.; Tharang, A.; Dettmann, S.; Roloff, A. Role of street trees in mitigating effects of heat and drought at highly sealed urban sites. *Landsc. Urban Plan.* **2015**, *143*, 33–42. [[CrossRef](#)]
29. Tan, Z.; Lau, K.K.-L.; Ng, E. Urban tree design approaches for mitigating daytime urban heat island effects in a high-density urban environment. *Energy Build.* **2016**, *114*, 265–274. [[CrossRef](#)]
30. Perini, K.; Chokhachian, A.; Dong, S.; Auer, T. Modeling and simulating urban outdoor comfort: Coupling ENVI-Met and TRNSYS by grasshopper. *Energy Build.* **2017**, *152*, 373–384. [[CrossRef](#)]
31. Öztürk, M. Complete intra-annual cycle of Leaf Area Index in a *Platanus orientalis* L. stand. *Plant Biosyst. Int. J. Deal. Asp. Plant Biol.* **2016**, *150*, 1296–1305.
32. Srivani, M.; Hokao, K. Evaluating the cooling effects of greening for improving the outdoor thermal environment at an institutional campus in the summer. *Build. Environ.* **2013**, *66*, 158–172. [[CrossRef](#)]
33. Georgi, N.; Zafiriadis, K. The impact of park trees on microclimate in urban areas. *Urban Ecosyst.* **2006**, *9*, 195–209. [[CrossRef](#)]
34. Technical Chamber of Greece. *Technical Guide TOTEE 20701-2*; Technical Chamber of Greece: Athens, Greece, 2017. (In Greek)
35. Guattari, C.; Evangelisti, L.; Balaras, C.A. On the assessment of urban heat island phenomenon and its effects on building energy performance: A case study of Rome (Italy). *Energy Build.* **2018**, *158*, 605–615. [[CrossRef](#)]
36. Ciancio, V.; Falasca, S.; Golasi, I.; Curci, G.; Coppi, M.; Salata, F. Influence of input climatic data on simulations of annual energy needs of a building: EnergyPlus and WRF modeling for a case study in Rome (Italy). *Energies* **2018**, *11*, 2835. [[CrossRef](#)]
37. *ISO 6946:2007*; Building Components and Building Elements—Thermal Resistance and Thermal Transmittance—Calculation Method. International Organization for Standardization: Geneva, Switzerland, 2007.
38. Simon, H.; Bruse, M.; Cramer, L.; Sinsel, T. Improving building performance simulation boundary conditions. In Proceedings of the 35th International Conference on Passive and Low Energy Architecture, Coruña, Spain, 1–3 September 2020.

Disclaimer/Publisher’s Note: The statements, opinions and data contained in all publications are solely those of the individual author(s) and contributor(s) and not of MDPI and/or the editor(s). MDPI and/or the editor(s) disclaim responsibility for any injury to people or property resulting from any ideas, methods, instructions or products referred to in the content.